chemistry

MDPI

*Supplementary*

# Unveiling the Unexpected Reactivity of Electrophilic Diazoalkanes in [3+2] Cycloaddition Reactions within Molecular Electron Density Theory

**Luis R. Domingo [1,*], Mar Ríos-Gutiérrez [1] and Nivedita Acharjee [2]**

[1] Department of Organic Chemistry, University of Valencia, Dr. Moliner 50, Burjassot, 46100 Valencia, Spain; rios@utopia.uv.es
[2] Department of Chemistry, Durgapur Government College, J. N. Avenue, Durgapur, West Bengal 713214, India; nivchem@gmail.com
* Correspondence: domingo@utopia.uv.es

**Index**

**1. BET study of the 32CA reaction of DAA 7 with NBD 11.**

Krokoidis [1] proposed the bonding evolution theory (BET) to structure the molecular mechanism of a chemical reaction by the conjunction of ELF topological study [2,3] and Thom's catastrophe [4]. The energy cost (EC) for the electron density changes along the reaction path are determined by BET within the Molecular electron Density Theory (MEDT) framework [5-7]. Herein, the BET study for the 32CA reaction of DAA **7** with NBD **11** is presented. Identification of catastrophe along this reaction allowed dividing into nine topological *phases*. The ELF valence basin populations, energy cost and GEDT at the identifying IRC points of each *phase* and pyrazoline **12** are given in Table S1.

*Phase I* starts at **S0-I** ($d_{N1-C5}$ = 3.02 Å, $d_{C3-C4}$ = 3.14 Å) with GEDT = 0.03 e. The ELF of **S0-I** is similar to the reagents **7** and **11**, except that the two monosynaptic basins V(N1) and V'(N1) integrating 3.78 e in **7** have merged into single monosynaptic basin V(N1) integrating 3.77 e in **S0-I**. The low GEDT value suggests minimal electronic flux between the two reacting frameworks at this point.

*Phase II* starts at **S1-I** ($d_{N1-C5}$ = 2.40 Å, $d_{C3-C4}$ = 2.34 Å) with GEDT = 0.10 e. At this point, the monosynaptic basin V(N2) integrating 1.26 e is created which is associated with the non-bonding electron density at the N2 nitrogen. The N1–N2 and C3–N2 bonding regions of the DAA framework are depopulated to accumulate this non-bonding electron density at N2. The disynaptic basins V(N1,N2) and V'(N1,N2) undergo depopulation from 3.75 e at **S0-I** to 3.33 e at **S1-I**. The disynaptic basin V(C3,N2) is depopulated from 3.04 e at **S0-I** to 2.32 e at **S1-I**, which mainly contributes to the formation of monosynaptic basin V(N2). The N1-N2 and C3-N2 bonding regions experience depopulation along the reaction path until the geometry is finally relaxed to pyrazoline **12**, while the non-bonding electron density at N2 increases progressively reaching the ELF basin population of 2.70 e in pyrazoline **12**. Note that GEDT increases from 0.03 e at **S0-I** to 0.10 e at **S1-I**, and the global electronic flux is predicted as forward electron density transfer [8] (FEDF) from DAA **7** to NBD **11** demanding the EC of 14.9 kcal $mol^{-1}$.

*Phase III* starts at **S2-I** ($d_{N1-C5}$ = 2.38 Å, $d_{C3-C4}$ = 2.31 Å) with GEDT = 0.10 e. At this point, the two disynaptic basins V(C4,C5) and V'(C4,C5) are merged into one V(C4,C5) basin indicating the rupture of C4–C5 double bond demanding energy cost of 15.4 kcal $mol^{-1}$, with the FEDF process of GEDT 0.10 e. **TS1** belongs to this phase, suggesting that the activation energy of this 32CA reaction is associated with the formation of lone pair electron density at N2 nitrogen and the rupture of C4–C5 double bond.

*Phase IV* starts at **S3-I** ($d_{N1-C5}$ = 2.27 Å, $d_{C3-C4}$ = 2.16 Å) and is associated with the formation of monosynaptic basin V(C4) integrating 0.24 e, associated with the formation of *pseudoradical* centre at C4, required for the formation of C3–C4 single bond. Note that the disynaptic basin V(C4,C5) is depopulated from 3.34 at **S2-I** to 3.08 e at **S3-I**, to create the *pseudoradical* centre at C4.

*Phase V* starts at **S4-I** ($d_{N1-C5}$ = 2.23 Å, $d_{C3-C4}$ = 2.10 Å) and is associated with the formation of monosynaptic basin V(C5) integrating 0.30 e, associated with the formation of *pseudoradical* centre at C5, which is required for the formation of N1–C5 single bond. Note that the disynaptic basin V(C4,C5) is depopulated from 3.08 at **S3-I** to 2.68 e at **S4-I**.

*Phase VI* starts at **S5-I** ($d_{N1-C5}$ = 2.20 Å, $d_{C3-C4}$ = 2.05 Å), identified by the formation of disynaptic basin V(C3,C4) integrating 1.36 e. At this point, the first C3–C4 bond formation begins which finally reaches the ELF basin population of 1.94 e in the cycloadduct **6**. Note that the C3–C4 bond is formed by the coupling of C3 and C4 *pseudoradical* centres, indicated by the disappearance of monosynaptic basins V(C3) and V(C4) at **S5-I**.

*Phase VII* starts at **S6-I** ($d_{N1-C5}$ = 2.14 Å, $d_{C3-C4}$ = 1.96 Å). At this point, the two disynaptic basins V(N1,N2) and V'(N1,N2) integrating 1.46 e and 1.45 e at **S5-I** are merged into one V(N1,N2) basin integrating 2.82 e at **S6-I**.

*Phase VIII* starts at **S7-I** ($d_{N1-C5}$ = 2.06 Å, $d_{C3-C4}$ = 1.85 Å), characterised by the splitting of the monosynaptic basin V(N1) into two monosynaptic basins V(N1) and V'(N1). Finally, *Phase XI* starts at **S8-I** ($d_{N1-C5}$ = 1.84 Å, $d_{C3-C4}$ = 1.63 Å), identified by the formation of

V(N1,C5) disynaptic basin integrating 1.51 e associated with the formation of the second N1–C5 bond at the distance of 1.84 Å by coupling of the *pseudoradical* centre at C5 and a part of non-bonding electron density at N1 nitrogen [6]. The molecular geometry is finally relaxed at $d_{N1–C5}$ = 1.46 Å, $d_{C3–C4}$ = 1.52 Å in pyrazoline **12**. The formation of the second N1–C5 bond begins when the first C3–C5 bond has been 93 % completed, suggesting a highly asynchronous process of bond formation.

**Table 1.** ELF valence basin populations, distances of the forming bonds, and relative[a] electronic energies of the IRC structures **S0-I**–**S8-I** defining the nine phases characterizing the molecular mechanism of the 32CA reaction of simplest DAA **7** and NBD **11**. Distances are given in angstroms, Å, and relative energies in kcal·mol$^{-1}$.

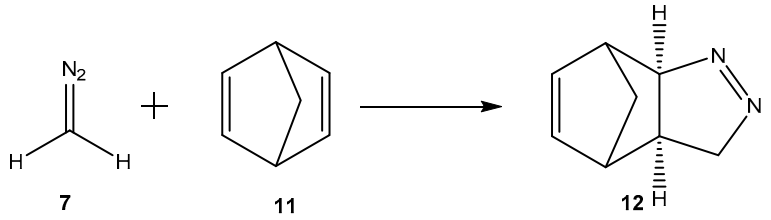


**7** **11** **12**

| *Phases* | *I* | *II* | *III* | *IV* | *V* | *VI* | *VII* | *VIII* | *IX* | |
|---|---|---|---|---|---|---|---|---|---|---|
| Structures | **S0-I** | **S1-I** | **S2-I** | **S3-I** | **S4-I** | **S5-I** | **S6-I** | **S7-I** | **S8-I** | **12** |
| d(N1–C5) | 3.02 | 2.40 | 2.38 | 2.27 | 2.23 | 2.20 | 2.14 | 2.06 | 1.84 | 1.46 |
| d(C3–C4) | 3.14 | 2.34 | 2.31 | 2.16 | 2.10 | 2.05 | 1.96 | 1.85 | 1.63 | 1.52 |
| ΔE | 0.0 | 14.9 | 15.4 | 15.0 | 13.0 | 10.6 | 5.2 | −4.7 | −29.0 | −53.5 |
| GEDT | 0.03 | 0.10 | 0.10 | 0.09 | 0.08 | 0.07 | 0.04 | 0.01 | 0.06 | 0.13 |
| V(N1) | 3.77 | 3.66 | 3.66 | 3.64 | 3.64 | 3.65 | 3.66 | 2.99 | 2.82 | 2.70 |
| V'(N1) | | | | | | | | 0.70 | | |
| V(N1,N2) | 1.88 | 1.66 | 1.63 | 1.51 | 1.49 | 1.46 | 2.82 | 2.76 | 2.65 | 2.52 |
| V'(N1,N2) | 1.87 | 1.67 | 1.64 | 1.53 | 1.46 | 1.45 | | | | |
| V(C3,N2) | 3.04 | 2.32 | 2.17 | 1.96 | 1.93 | 1.91 | 1.87 | 1.84 | 1.80 | 1.80 |
| V(C3) | 0.41 | 0.81 | 0.83 | 0.90 | 0.93 | | | | | |
| V'(C3) | 0.42 | | | | | | | | | |
| V(N2) | | 1.26 | 1.47 | 1.97 | 2.11 | 2.20 | 2.34 | 2.46 | 2.62 | 2.70 |
| V(C4,C5) | 1.73 | 1.66 | 3.34 | 3.08 | 2.68 | 2.54 | 2.36 | 2.23 | 2.03 | 1.91 |
| V'(C4,C5) | 1.73 | 1.69 | | | | | | | | |
| V(C4) | | | | 0.24 | 0.35 | | | | | |
| V(C5) | | | | | 0.30 | 0.37 | 0.47 | 0.52 | | |
| V(C3,C4) | | | | | | 1.36 | 1.48 | 1.59 | 1.81 | 1.94 |
| V(N1,C5) | | | | | | | | | 1.51 | 1.84 |

## 2. BET study of the 32CA reaction of DAA 10 with NBD 11

Identification of catastrophe along the 32CA reaction of DAA **10** with NBD **11** allows dividing the reaction into seven ELF topological *phases*. The ELF valence basin populations, energy cost and GEDT at the identifying IRC points of each *phase* and pyrazoline **22** are given in Table S2.

*Phase I* starts at **S0-II** ($d_{N1-C5}$ = 3.07 Å, $d_{C3-C4}$ = 3.02 Å) with GEDT = 0.02 e. The ELF of **S0-II** is similar to DAA **10** with NBD **11**. The low GEDT value suggests minimal electronic flux between the two reacting frameworks at this point.

*Phase II* starts at **S1-II** ($d_{N1-C5}$ = 2.29 Å, $d_{C3-C4}$ = 2.48 Å) with GEDT = 0.03 e and EC is 18.6 kcal $mol^{-1}$. At this point, the monosynaptic basin V(N2) integrating 1.03 e is created which is associated with the non-bonding electron density at the N2 nitrogen. The N1-N2 and C3–N2 bonding regions of the diazoalkane framework are depopulated to accumulate this non-bonding electron density at N2. The disynaptic basins V(N1,N2) and V'(N1,N2) undergo depopulation from 4.02 e at **S0-II** to 3.46 e at **S1-II**. The disynaptic basin V(C3,N2) is depopulated from 2.82 e at **S0-II** to 2.47 e at **S1-II**. The N1-N2 and C3-N2 bonding regions experience depopulation along the reaction path until the geometry is finally relaxed to pyrazoline **22**, while the non-bonding electron density at N2 increases progressively reaching the basin population of 2.69 e in pyrazoline **22**. Note that GEDT at **S1-II** is 0.03 e suggests minimal electronic flux between the two reacting frameworks.

*Phase III* starts at **S2-II** ($d_{N1-C5}$ = 2.22 Å, $d_{C3-C4}$ = 2.42 Å) with GEDT = 0.01 e. At this point, the two disynaptic basins V(C4,C5) and V'(C4,C5) are merged into one V(C4,C5) basin indicating the rupture of C4–C5 double bond demanding energy cost of 20.9 kcal $mol^{-1}$, with GEDT 0.01 e. **TS6** belongs to this phase, suggesting that the activation energy of this 32CA reaction is associated with the formation of lone pair electron density at N2 nitrogen and the rupture of C4–C5 double bond. It is worth mentioning that this phase begins with a GEDT value of 0.01 e at **S2-II**, reaching 0.04 e at **TS11**, classifying this 32CA reaction of NEDF. The EC demanded for reach **S2-II**, 20.9 kcal $mol^{-1}$, accounts for the high activation energy associated to this 32CA reaction, 23.3 kcal $mol^{-1}$.

*Phase IV* starts at **S3-II** ($d_{N1-C5}$ = 2.02 Å, $d_{C3-C4}$ = 2.23 Å) and is associated with the formation of monosynaptic basin V(C4) and V(C5) basins integrating 0.18 e and 0.27 e respectively, associated with the formation of *pseudoradical* centres at C4 and C5, required for the formation of C3–C4 and N1–C5 single bonds. Note that the disynaptic basin V(C4,C5) is depopulated from 3.26 at **S2-II** to 2.72 e at **S3-II**, to create the *pseudoradical* centres at C4 and C5.

*Phase V* starts at **S4-II** ($d_{N1-C5}$ = 1.93 Å, $d_{C3-C4}$ = 2.15 Å), characterised by the splitting of the monosynaptic basin V(N1) integrating 3.51 e into two monosynaptic basins V(N1) and V'(N1) integrating 2.98 e and 0.60 e respectively.

*Phase VI* starts at **S5-II** ($d_{N1-C5}$ = 1.89 Å, $d_{C3-C4}$ = 2.11 Å), identified by the formation of disynaptic basin V(C3,C4) integrating 1.25 e. At this point, the first C3–C4 bond formation begins which finally reaches the ELF basin population of 1.95 e in pyrazoline **22**. Note that the C3–C4 bond formed by the coupling of C3 and C4 *pseudoradical* centres, indicated by the disappearance of monosynaptic basins V(C3) and V(C4) at **S5-II**.

Finally, *Phase VII* starts at **S6-II** ($d_{N1-C5}$ = 1.82 Å, $d_{C3-C4}$ = 2.03 Å), identified by the formation of V(N1,C5) disynaptic basin integrating 1.38 e associated with the formation of the second N1–C5 bond at the distance of 1.82 Å by coupling of the *pseudoradical* centre at C5 and a part of non-bonding electron density at N1 nitrogen [6]. The molecular geometry is finally relaxed at $d_{N1-C5}$ = 1.46 Å, $d_{C3-C4}$ = 1.53 Å in pyrazoline **22**. The formation of the second N1–C5 bond begins when the first C3–C5 bond has been 70 % completed, suggesting a less asynchronous process relative to that observed in the 32CA reaction of DAA **10** with NBD **11**.

**Table 2.** ELF valence basin populations, distances of the forming bonds, and relative[a] electronic energies of the IRC structures **S0-II**–**S6-II** defining the seven phases characterizing the molecular mechanism of the 32CA reaction of DAA **10** and NBD **11.** Distances are given in angstroms, Å, and relative energies in kcal·mol$^{-1}$.

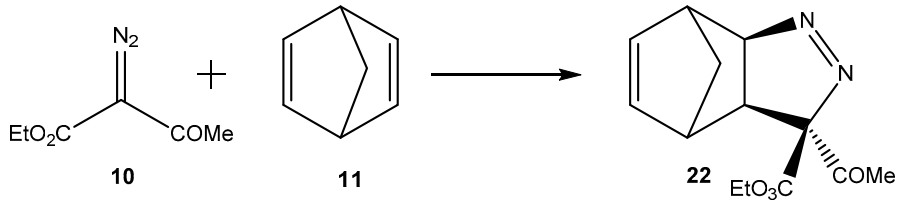


| *Phases* | *I* | *II* | *III* | *IV* | *V* | *VI* | *VII* | |
|---|---|---|---|---|---|---|---|---|
| Structures | **S0-II** | **S1-II** | **S2-II** | **S3-II** | **S4-II** | **S5-II** | **S6-II** | **22** |
| d(N1–C5) | 3.07 | 2.29 | 2.22 | 2.02 | 1.93 | 1.89 | 1.82 | 1.46 |
| d(C3–C4) | 3.02 | 2.48 | 2.42 | 2.23 | 2.15 | 2.11 | 2.03 | 1.53 |
| ΔE | 0.0 | 18.6 | 20.9 | 22.4 | 19.4 | 16.9 | 11.4 | -30.0 |
| GEDT | 0.02 | 0.03 | 0.01 | 0.08 | 0.11 | 0.13 | 0.15 | 0.19 |
| V(N1) | 3.43 | 3.40 | 3.41 | 3.51 | 2.98 | 2.85 | 2.78 | 2.65 |
| V'(N1) | | | | | 0.60 | 0.77 | | |
| V(N1,N2) | 2.14 | 2.01 | 1.93 | 1.71 | 2.85 | 2.80 | 2.74 | 2.56 |
| V'(N1,N2) | 1.88 | 1.45 | 1.37 | 1.25 | | | | |
| V(C3,N2) | 2.82 | 2.47 | 2.22 | 1.97 | 1.95 | 1.94 | 1.94 | 1.81 |
| V(C3) | 0.29 | 0.55 | 0.62 | 0.79 | 0.85 | | | |
| V'(C3) | 0.59 | | | | | | | |
| V(N2) | | 1.03 | 1.45 | 2.12 | 2.28 | 2.36 | 2.44 | 2.69 |
| V(C4,C5) | 1.74 | 1.64 | 3.26 | 2.72 | 2.47 | 2.38 | 2.26 | 1.91 |
| V'(C4,C5) | 1.72 | 1.68 | | | | | | |
| V(C4) | | | | 0.18 | 0.32 | | | |
| V(C5) | | | | 0.27 | 0.41 | 0.45 | | |
| V(C3,C4) | | | | | | 1.25 | 1.36 | 1.95 |
| V(N1,C5) | | | | | | | 1.38 | 1.85 |

**References.**


1. Krokidis, X.; Noury, S.; Silvi, B. Characterization of Elementary Chemical Processes by Catastrophe Theory. *J. Phys. Chem. A.*, **1997**, *101*, 7277. https://doi.org/10.1021/jp9711508
2. Becke, A.D.; Edgecombe, K.E. A simple measure of electron localization in atomic and molecular systems, *J. Chem. Phys.* **1990**, *92*, 5397–5403. https://doi.org/10.1063/1.458517
3. Silvi, B.; Savin, A. Classification of chemical bonds based on topological analysis of electron localization functions, *Nature* 1994, *371*, 683–686. https://www.nature.com/articles/371683a0
4. Thom, R. *Stabilité Structurelle et Morphogénèse*; Intereditions, Paris, **1972**
5. Domingo, L.R. Molecular electron density theory. *Molecules.* **2016**, *21*, 1319. https://doi.org/10.3390/molecules21101319
6. Ríos-Gutiérrez, M.; Domingo, L.R. Unravelling the mysteries of the [3+2] cycloaddition reactions. *Eur. J. Org. Chem*. **2019**, 267–282. https://doi.org/10.1002/ejoc.201800916
7. Domingo, L.R.; Acharjee, N. Molecular Electron Density Theory: A New Theoretical Outlook on Organic Chemistry. in *Frontiers in Computational Chemistry*, Bentham and Science (Ed. Z. Ul-Haq, A. K. Wilson), Singapore, **2020**, *5*, 174-227. https://doi.org/10.2174/9789811457791120050007
8. Domingo, L.R.; Ríos-Gutiérrez, M.; Pérez. P. A molecular electron density theory study of the participation of tetrazines in aza-Diels–Alder reactions. *RSC Adv.* 2020, *10*, 15394-15405. https://doi.org/10.1039/D0RA01548B

**Table 3.** MPWB1K/6-311G(d,p) electronic chemical potential $\mu$, chemical hardness $\eta$, electrophilicity $\omega$ and nucleophilicity $N$ indices, in eV, of DAAs **7**-**10** and NBD **11**.

| | μ | η | ω | *N* |
|---|---|---|---|---|
| DAA**10** | −4.52 | 7.23 | 1.41 | 2.26 |
| DAA **8** | −4.33 | 6.73 | 1.39 | 2.71 |
| DAA **9** | −4.18 | 7.15 | 1.22 | 2.64 |
| DAA **7** | −3.55 | 7.10 | 0.89 | 3.30 |
| NBD **11** | −3.23 | 7.83 | 0.66 | 3.26 |

**Table 4.** MPWB1K/6-311G(d,p) calculated gas phase total energies (au), enthalpies (au), entropies (cal mol$^{-1}$ K$^{-1}$) and Gibbs free energies (au), computed at 298 K, of the stationary points involved in the 32CA reactions of DAAs **7–10**, with NBD **11.**

| | E | H | S | G |
|---|---|---|---|---|
| **7** | −148.69435 | −148.657068 | 58.873 | -148.68504 |
| **8** | −415.844663 | -415.72723 | 89.001 | -415.769517 |
| **9** | −493.007389 | -492.869224 | 95.64 | -492.914666 |
| **10** | −568.466717 | −568.30722 | 107.406 | −568.358252 |
| **11** | −271.404078 | −271.266391 | 69.543 | −271.299433 |
| **TS1** | −420.073079 | −419.896687 | 86.141 | −419.937615 |
| **12** | −420.183805 | −420.001483 | 81.086 | −420.040009 |
| **TS2** | −420.072024 | −419.895795 | 85.499 | −419.936418 |
| **13** | −420.182658 | −420.000379 | 80.875 | −420.038806 |
| **TS3** | −687.218670 | −686.962688 | 116.244 | −687.017919 |
| **14** | −687.318889 | −687.057769 | 112.029 | −687.110998 |
| **TS4** | −687.213751 | −686.95766 | 114.422 | −687.012026 |
| **15** | −687.315871 | −687.054554 | 109.346 | −687.106508 |
| **TS5** | −687.217623 | −686.961532 | 115.995 | −687.016645 |
| **16** | −687.321001 | −687.059564 | 111.168 | −687.112384 |
| **TS6** | −687.216211 | −686.960401 | 117.184 | −687.016079 |
| **17** | −687.318993 | −687.057956 | 115.091 | −687.112639 |
| **TS7** | −764.377342 | −764.100582 | 119.285 | −764.157258 |
| **18** | −764.475762 | −764.194883 | 110.135 | −764.247211 |
| **TS8** | −764.375875 | −764.098805 | 116.898 | −764.154346 |
| **19** | −764.474433 | −764.19222 | 113.000 | −764.24591 |
| **TS9** | −764.376856 | −764.099803 | 118.229 | −764.155977 |
| **20** | −764.47724 | −764.195036 | 114.649 | −764.249509 |
| **TS10** | −764.378599 | −764.102027 | 119.173 | −764.15865 |
| **21** | −764.482603 | −764.200579 | 114.079 | −764.254782 |
| **TS11** | −839.833689 | −839.535002 | 129.212 | −839.596395 |
| **22** | −839.918716 | −839.616332 | 128.989 | −839.677619 |
| **TS12** | −839.829094 | −839.530588 | 128.497 | −839.591641 |
| **23** | −839.926699 | −839.624244 | 127.09 | −839.684629 |
| **TS13** | −839.832754 | −839.535015 | 130.981 | −839.597249 |
| **24** | −839.924998 | −839.622756 | 133.848 | −839.686352 |
| **TS14** | −839.828571 | −839.530332 | 127.416 | −839.590872 |
| **25** | −839.921068 | −839.618605 | 126.33 | −839.678629 |

**Table 5.** MPWB1K/6-311G(d,p) calculated total energies (au), enthalpies (au), entropies (cal $mol^{-1}$ $K^{-1}$) and Gibbs free energies (au) at 298 K in acetonitrile, of the stationary points involved in the 32CA reactions of DAAs **7–10**, with NBD **11.**

| | E | H | S | G |
|---|---|---|---|---|
| **7** | −148.697971 | −148.660962 | 57.47 | −148.688268 |
| **8** | −415.853846 | −415.737226 | 89.747 | −415.779867 |
| **9** | −493.021776 | −492.884693 | 95.538 | −492.930087 |
| **10** | −568.476852 | −568.317887 | 107.191 | −568.368817 |
| **11** | −271.409144 | −271.27258 | 69.619 | −271.305658 |
| **TS1** | −420.080447 | −419.90526 | 86.266 | −419.946248 |
| **12** | −420.195714 | −420.014475 | 81.136 | −420.053025 |
| **TS2** | −420.079059 | −419.903991 | 85.492 | −419.944611 |
| **13** | −420.195114 | −420.013908 | 80.956 | −420.052373 |
| **TS3** | −687.231098 | −686.976676 | 116.894 | −687.032217 |
| **14** | −687.336732 | −687.076882 | 111.144 | −687.12969 |
| **TS4** | −687.225838 | −686.971464 | 115.409 | −687.026298 |
| **15** | −687.335209 | −687.075452 | 110.167 | −687.127795 |
| **TS5** | −687.229657 | −686.974992 | 115.26 | −687.029756 |
| **16** | −687.336792 | −687.076919 | 112.92 | −687.130571 |
| **TS6** | −687.228138 | −686.973966 | 116.932 | −687.029524 |
| **17** | −687.336102 | −687.076454 | 113.571 | −687.130415 |
| **TS7** | −764.393769 | −764.118933 | 118.12 | −764.175056 |
| **18** | −764.493208 | −764.213033 | 122.807 | −764.271382 |
| **TS8** | −764.392628 | −764.117971 | 118.865 | −764.174447 |
| **19** | −764.498509 | −764.217877 | 112.944 | −764.27154 |
| **TS9** | −764.392619 | −764.117578 | 118.400 | −764.173834 |
| **20** | −764.496626 | −764.216391 | 115.619 | −764.271326 |
| **TS10** | −764.394578 | −764.119827 | 119.264 | −764.176493 |
| **21** | −764.500661 | −764.220645 | 115.062 | −764.275315 |
| **TS11** | −839.848424 | −839.551108 | 129.03 | −839.612414 |
| **22** | −839.940461 | −839.63928 | 128.472 | −839.700321 |
| **TS12** | −839.843494 | −839.546462 | 128.895 | −839.607704 |
| **23** | −839.943924 | −839.642831 | 125.585 | −839.702501 |
| **TS13** | −839.847954 | −839.550908 | 130.712 | −839.613013 |
| **24** | −839.943531 | −839.642447 | 128.169 | −839.703345 |
| **TS14** | −839.843147 | −839.545945 | 126.185 | −839.605899 |
| **25** | −839.940838 | −839.639635 | 127.604 | −839.700263 |